Advances in Laser Cooling of Semiconductors

M. Sheik-Bahae[(a)], B. Imangholi[(a)], M. P. Hasselbeck[(a)], R. I. Epstein[(a,b)], S. Kurtz[(c)]

(a) Department of Physics and Astronomy, University of New Mexico, Albuquerque, NM, 87131
(505) 277-2080, msb@unm.edu
(b) Los Alamos National Laboratories, Los Alamos, NM
(c) National Renewable Energy Laboratory, Golden, CO 80401 USA

ABSTRACT

Laser cooling in semiconductor structures due to anti-Stokes luminescence is reviewed. Theoretical background considering luminescence trapping and red-shifting, the effect of free carrier and back-ground absorption, Pauli band-blocking, and the temperature-dependence of various recombination mechanisms are discussed. Recent experimental results demonstrating record external quantum efficiencies (EQE) in GaAs/GaInP heterostructures are described, and conditions favorable for the first observation of laser cooling in semiconductors are discussed.
Keywords: laser cooling, semiconductors, optical refrigeration, external quantum efficiency

1. INTRODUCTION

The principle of laser cooling (optical refrigeration) by means of luminescence upconversion in solids dates back to 1929 when Pringsheim recognized that thermal vibrational energy can be removed by anti-Stokes fluorescence if the material is excited by light whose photon energy is below its mean fluorescence[1].(See Fig. 1) The first observation of laser cooling in a solid was in highly pure ytterbium doped glass in 1995 [2] followed by a similar report of laser cooling phenomena in a dye solution [3]. Since then numerous investigations of laser cooling involving ytterbium and thulium atoms in various host materials have been reported.[4-9] A temperature drop of $\Delta T \approx 70$ K from room temperature has been obtained, and proposals have been made to employ this phenomenon for an all-solid-state cryocooler application.[5] In parallel, there have been a number of experimental investigations of laser cooling in semiconductors although no net cooling has been observed. This is primarily due to luminescence trapping.[10, 11] The theoretical aspects of cooling in semiconductors have been tackled by a number of authors, but early work did not systematically address many practical issues such as luminescence trapping and red-shifting or band-blocking effects.[12, 13]

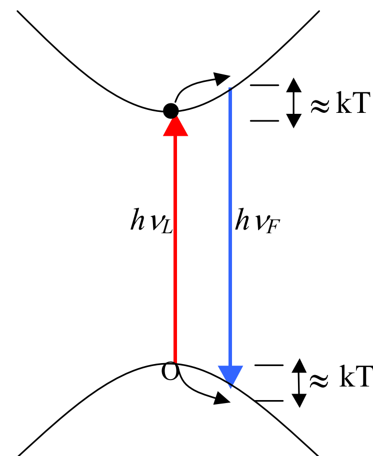

Fig 1. Cooling cycle in laser refrigeration of a semiconductor in which a laser photon with energy hν is absorbed following by an up-converted luminescence at $h\nu_F$.

Among the advantages of semiconductors over rare-earth doped solids is their potential for achieving very low (≈ 10 K) temperatures. This stems from the difference in the ground state population distribution in the two systems. As the temperature a rare-earth doped system is lowered to 100 K and below, the population at the top of the ground state manifold (following Boltzmann statistics) begins to vanish, thus rendering the cooling cycle highly inefficient. In semiconductors, the

Report Documentation Page

Form Approved
OMB No. 0704-0188

Public reporting burden for the collection of information is estimated to average 1 hour per response, including the time for reviewing instructions, searching existing data sources, gathering and maintaining the data needed, and completing and reviewing the collection of information. Send comments regarding this burden estimate or any other aspect of this collection of information, including suggestions for reducing this burden, to Washington Headquarters Services, Directorate for Information Operations and Reports, 1215 Jefferson Davis Highway, Suite 1204, Arlington VA 22202-4302. Respondents should be aware that notwithstanding any other provision of law, no person shall be subject to a penalty for failing to comply with a collection of information if it does not display a currently valid OMB control number.

1. REPORT DATE	2. REPORT TYPE	3. DATES COVERED
2006		**00-00-2006 to 00-00-2006**

4. TITLE AND SUBTITLE
Advances in Laser Cooling of Semiconductors

5a. CONTRACT NUMBER
5b. GRANT NUMBER
5c. PROGRAM ELEMENT NUMBER

6. AUTHOR(S)

5d. PROJECT NUMBER
5e. TASK NUMBER
5f. WORK UNIT NUMBER

7. PERFORMING ORGANIZATION NAME(S) AND ADDRESS(ES)
University of New Mexico,Department of Physics and Astronomy,Albuquerque,NM,87131

8. PERFORMING ORGANIZATION REPORT NUMBER

9. SPONSORING/MONITORING AGENCY NAME(S) AND ADDRESS(ES)

10. SPONSOR/MONITOR'S ACRONYM(S)

11. SPONSOR/MONITOR'S REPORT NUMBER(S)

12. DISTRIBUTION/AVAILABILITY STATEMENT
Approved for public release; distribution unlimited

13. SUPPLEMENTARY NOTES
Proceedings of SPIE, Photonics West (2006)

14. ABSTRACT
Laser cooling in semiconductor structures due to anti-Stokes luminescence is reviewed. Theoretical background considering luminescence trapping and red-shifting, the effect of free carrier and back-ground absorption, Pauli bandblocking and the temperature-dependence of various recombination mechanisms are discussed. Recent experimental results demonstrating record external quantum efficiencies (EQE) in GaAs/GaInP heterostructures are described, and conditions favorable for the first observation of laser cooling in semiconductors are discussed.

15. SUBJECT TERMS

16. SECURITY CLASSIFICATION OF:			17. LIMITATION OF ABSTRACT	18. NUMBER OF PAGES	19a. NAME OF RESPONSIBLE PERSON
a. REPORT	b. ABSTRACT	c. THIS PAGE			
unclassified	**unclassified**	**unclassified**	**Same as Report (SAR)**	**13**	

Standard Form 298 (Rev. 8-98)
Prescribed by ANSI Std Z39-18

population in the valence band (See Fig. 1) obeys Fermi-Dirac statistics. A mid-gap Fermi energy implies high occupation even at T=0.

In this paper, we present a theoretical foundation of laser cooling in a semiconductor structures with an arbitrary external efficiency. This treatment for the first time accounts for the luminescence red-shift due to re-absorption. We then combine this theory with the well known plasma theory of semiconductors accounting for many body Coulomb effects and Pauli band-blocking to obtain the favorable conditions for observing laser cooling in bulk semiconductor heterostructures. We then discuss the latest experimental results toward the first observation of laser cooling in a semiconductor material.

2. THEORETICAL BACKGROUND

The system we investigate is an intrinsic (undoped) semiconductor system uniformly irradiated with a laser light at photon energy $h\nu$. Furthermore, we assume that only a fraction η_e of the luminescence can escape the material while the remaining fraction $(1-\eta_e)$ is trapped and re-absorbed, thus contributing to carrier generation. Under steady-state conditions at a given temperature the electron-hole (e-h) carrier density (N) is obtained from

$$0 = \frac{dN}{dt} = \frac{\alpha(\nu, N)}{h\nu} I - AN - BN^2 - CN^3 + (1-\eta_e)BN^2 \quad (1)$$

Here $\alpha(\nu,N)$ is the interband absorption coefficient that in general includes all the many-body and blocking factors. The recombination process consists primarily of nonradiative (AN), radiative (BN^2) and Auger (CN^3) recombination rates. All the above coefficients are temperature dependent. The density-dependence of α results from both Coulomb screening and Pauli-blocking (saturation) effects. The latter can be approximated by a blocking factor such that [14, 15]:

$$\alpha\,(N, h\nu) = \alpha_0(N, h\nu)\{f_v - f_c\} \quad (2)$$

where α_0 denotes the unsaturated absorption coefficient and the strongly density-dependent blocking factor [16] contains Fermi-Dirac distribution functions for the valence and conduction bands.

Eq. (1) can be re-written as

$$0 = \frac{\alpha(\nu, N)}{h\nu} I - AN - \eta_e BN^2 - CN^3 \quad (3)$$

This indicates that the florescence trapping effectively inhibits the spontaneous emission as it appears through η_eB only. This result has also been shown previously by Asbeck [17]. It is important to note that η_e is itself an averaged quantity over the entire luminescence spectrum.

$$\eta_e = \frac{\int S(\nu)R(\nu)d\nu}{\int R(\nu)d\nu}. \quad (4)$$

Here $S(\nu)$ is the geometry-dependent escape probability of photons with energy $h\nu$ and $R(\nu)$ is the luminescence spectral density that is related to the absorption coefficient through reciprocity using a "non-equilibrium" van Roosbroeck-Shockley relation (also known as Kubo-Martin-Schwinger (KMS) relation) [14, 18]:

$$R(\nu, N) = \frac{8\pi n^2 \nu^2}{c^2} \alpha\,(\nu, N) \left\{ \frac{f_c(1-f_v)}{f_v - f_c} \right\}, \quad (5)$$

where c is the speed of light and n is the index of refraction. Note that radiative recombination coefficient B is obtained by $BN^2 = \int R(\nu)d\nu$ which results in a negligible dependence of B on N at carrier densities of interest. The net power density that is deposited in the semiconductor is the difference between the power densities absorbed from the laser and that of the luminescence that escapes:

$$P_{net} = \alpha I + \int (1 - S(\nu))R(\nu)h\nu d\nu + \Delta P - \int R(\nu)h\nu d\nu \,. \quad (6)$$

The first two terms in equation (6) include absorption contributions from laser and trapped luminescence and contribute to heating. The fourth term accounts for emission that has a cooling contribution. An extra heating term ΔP is included to account for the effects such as free-carrier absorption and other parasitic absorptive processes. With the aid of Equation (3), we rewrite Equation (6) as:

$$P_{net} = \eta_e BN^2(h\nu - h\tilde{\nu}_f) + ANh\nu + CN^3 h\nu + \Delta P \,, \quad (7)$$

where we have defined an "escaped" mean luminescence photon energy as

$$h\tilde{\nu}_f = \frac{\int S(\nu)R(\nu)h\nu d\nu}{\int S(\nu)R(\nu)d\nu} \,. \quad (8)$$

Equation (7) rigorously describes laser cooling of a semiconductor in a compact and simple form. It accounts for the practical considerations of luminescence trapping by introducing an inhibited radiative recombination (η_e B) and a shifted mean photon energy $h\tilde{\nu}_f$ for the escaped luminescence. For high external efficiency systems where S(ν)=1, Equation (7) approaches that described in the literature with η_e=1 and $\tilde{\nu}_f = \nu_f$ with ν_f denoting the mean fluorescence energy produced internally in the semiconductor[11-13]. Equation (7) indicates that laser cooling occurs when $P_{net} < 0$, requiring a dominant contribution from the radiative recombination with $h\nu < h\tilde{\nu}_f$. The cooling efficiency η_c is defined as the ratio of cooling power density P_c ($=-P_{net}$) to the absorbed laser power density ($P_{abs}=\alpha I+\Delta P$). With the aid of Equation (3), this efficiency can be expressed as

$$\eta_c = -\frac{\eta_e BN^2(h\nu - h\tilde{\nu}_f) + ANh\nu + CN^3 h\nu + \Delta P}{\eta_e BN^2 h\nu + ANh\nu + CN^3 h\nu + \Delta P} \,. \quad (9)$$

Ignoring the ΔP contributions for the moment, η_c can be written more simply as:

$$\eta_c = \eta_{ext}\frac{\tilde{\nu}_f}{\nu} - 1 \,, \quad (10)$$

where η_{ext} describes the *external* quantum efficiency:

$$\eta_{ext} = \frac{\eta_e BN^2}{AN + \eta_e BN^2 + CN^3} \approx (\eta_i)^{1/\eta_e} \,, \quad (11)$$

with $\eta_i = BN^2/(AN+BN^2+CN^3)$ denoting the *internal* quantum efficiency [11, 19]. Including background parasitic absorption ($\Delta P=\alpha_b I$), results in a general form of cooling efficiency:

$$\eta_c = \eta_{abs}\eta_{ext}\frac{\tilde{\nu}_f}{\nu} - 1, \quad (12)$$

where the absorption efficiency η_{abs} is defined as the fraction of total absorbed photons (in the whole system including the substrate) that is consumed by the resonant absorption in the cooling (active) region:

$$\eta_{abs} = \frac{\alpha(\nu)}{\alpha(\nu)+\alpha_b} \quad .(13)$$

Note that we have assumed α_b is broadband and does not vary drastically in the vicinity of the band-edge region.

The above formalism as summarized by Equation (7). Ignoring ΔP, the roots of equation (7) leads to the carrier density limits within which net cooling can be observed provided that $\eta_e B(h\tilde{\nu}_f - h\nu) \geq 2h\nu\sqrt{AC}$ with the equal sign implying the break-even condition. Assuming radiative recombination dominates (i.e. the carrier density N is chosen such that $\eta_e B/C > N > A/\eta_e B$) and ignoring the band-blocking, one can solve for the incident laser irradiance. Within the above approximation, we can also account for parasitic absorption by taking $\Delta P=\alpha_b I+\sigma_{fca} NI$ where α_b denotes an *effective* background parasitic absorption as before and σ_{fca} is the free-carrier-absorption cross section. In this case, net cooling can occur within an irradiance range of $I_1 < I < I_2$ where $I_{1,2} = (h\nu\eta_e B/\alpha(\nu))N_{1,2}^2$ and

$$N_{1,2} = \left(\eta_q - \frac{\alpha_b}{\alpha(\nu)}\right)\frac{\eta_e B}{2C'}\left(1 \mp \sqrt{1-\frac{A}{A_0}}\right). \quad (14)$$

Here $\eta_q = \frac{h\tilde{\nu}_f - h\nu}{h\nu}$ denotes the quantum cooling efficiency, $C' = C + \sigma_{fca}\eta_e B/\alpha(\nu)$, and

$$A_0 = \left(\eta_q - \frac{\alpha_b}{\alpha(\nu)}\right)^2 \frac{(\eta_e B)^2}{4C'} \quad (15)$$

is the break-even (maximum allowable) nonradiative decay rate. For incident Gaussian laser beams, one can show that spatial averaging can be taken into account by multiplying A and C' by 2 and 2/3 respectively.

The parameters B and C are fundamental properties of a semiconductor and can be calculated for bulk or quantum-confined structures. The reported values for these coefficients, however, vary considerably. In bulk GaAs, for example, the published values are $2\times10^{-16} < B < 7\times10^{-16}$ and $1\times10^{-42} < C < 7\times10^{-42}$ in MKS units . These variations are primarily due to experimental uncertainties. We assume average values of $B = 4\times10^{-16}$ and $C = 4\times10^{-42}$ MKS, while ignoring the effects of background and free carrier absorption. These assumptions allow us to gain insight into the feasibility and requirements for achieving net laser cooling, It should be noted that the theoretical values for these parameters, depending on the complexity of the models used, vary almost within the same range as the experimental results. For example, a simple two-band model (as is used here) gives $B \approx 5\times10^{-16}$ MKS [20]. Using Equation (15), we plot in Figure 2 the break-even nonradiative lifetime $\tau_{nr}^0=A_0^{-1}$ as η_e varies assuming $h\nu_f$-$h\nu$=kT with $\hbar\nu_f$ corresponding to $\lambda_f \approx 860$ nm at room temperature. The gray area under the curve is the unwanted (heating) zone. The horizontal line corresponding to $\tau_{nr}\approx40$ μs is the longest reported nonradiative lifetime in a GaAs/InGaP double heterostructure; typical attainable lifetimes in such high quality structures are lower than this value (i.e. between 5-10 μs)[21]. Keeping this lifetime range in mind, we note that the lower limit on extraction efficiency (η_e) is 15% while in practice 25-30% may be required. Equation (15) also suggests that increasing the quantum efficiency η_q by decreasing the incident photon energy (e.g. at $h\nu_f$- $h\nu$>kT) relaxes this requirement. Interband absorption drops rapidly as the excitation moves further in the Urbach tail and one may no longer ignore background and free carrier absorption. Recently, it was found that FCA at the band edge wavelengths is much smaller than previously expected [22, 23]. For GaAs, $\sigma_{FCA}\approx10^{-24}$ m^2 [22, 23], which requires $\alpha(\nu)\geq10^3$ m^{-1} to ensure that free carrier losses are negligible (i.e. C'≈C). This requirement is satisfied even at λ = 890 nm (corresponding to $h\nu_f$-$h\nu\approx$2kT) where $\alpha(\nu) \approx10^4$ m^{-1}. We conclude that FCA does not pose a limitation on laser cooling. The possible sources of significant α_b are (a) impurity absorption in active material and/or the cladding layers of the heterostructures and (b) substrate absorption. It is also implicit that α_b in Equation (15) is scaled such that the actual background absorption coefficient $\alpha'_b=\alpha_b\times(d/L)$, where d and L are the thicknesses of the loss and active media (if

different) respectively. For example, for an active medium with L ≈ 1 μm and a substrate thickness of 1 cm, this requires $\alpha(\nu)>10^5\alpha'_b$. This, in turn demands $\alpha'_b<10\ \mathrm{m^{-1}}$ at λ=870 nm, and $\alpha'_b<0.1\ \mathrm{m^{-1}}$ at λ=890 nm. A ZnS substrate with $\alpha'_b\approx10^{-2}\ \mathrm{m^{-1}}$ meets such a requirement while ZnSe having $\alpha'_b\approx0.3\ \mathrm{m^{-1}}$ can only be effective at λ≈870 nm [24]. We shall later discuss the substrate issues and their role as index-matching domes for enhancing η_e. Before proceeding, it is instructive to show an alternative and compact way of expressing the cooling condition. Since optimum carrier density occurs at $N_{op}=(A/C)^{1/2}$, we can take $h\nu_f-h\nu=kT$ and write the cooling condition is to satisfy

$$\eta_{ext}\approx1-\frac{2\sqrt{AC}}{\eta_e B}>1-\frac{kT}{E_g}+\frac{\alpha_b}{\alpha_r(\nu)} \quad (16)$$

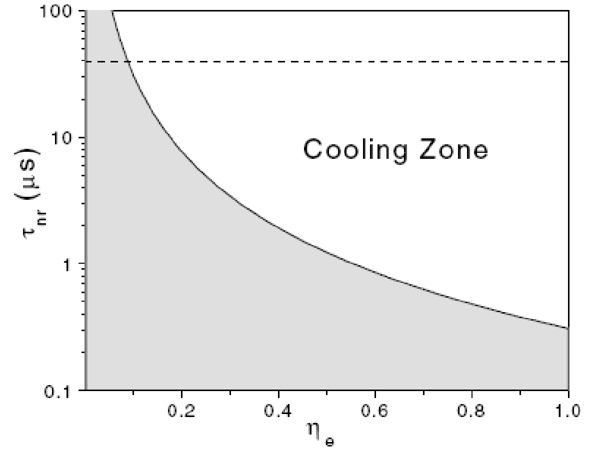

Fig. 2 The break-even nonradiative lifetime as a function of the luminescence extraction efficiency in bulk GaAs. The Horizontal line corresponds to $\tau_{nr}\approx40$ μs, the longest lifetime reported in a GaAs/InGaP double heterostructure.

Our analysis so far has been only concerned with net cooling from room temperature. Scaling the break-even condition to cryogenic temperatures is also of key importance. Using the expected scaling for $C(T)\propto\exp(-\beta(300/T-1))$ with β≈2.4 for GaAs [25, 26], $B\propto T^{-3/2}$ [14, 27], keeping $\eta_q\approx kT/E_g$ and ignoring parasitic losses and the small temperature dependence of the band-gap energy we obtain

$$\frac{A_0(T)}{A_0(300)}\approx\left(\frac{300}{T}\right)\exp\left(\frac{\beta(300-T)}{T}\right) \quad (17)$$

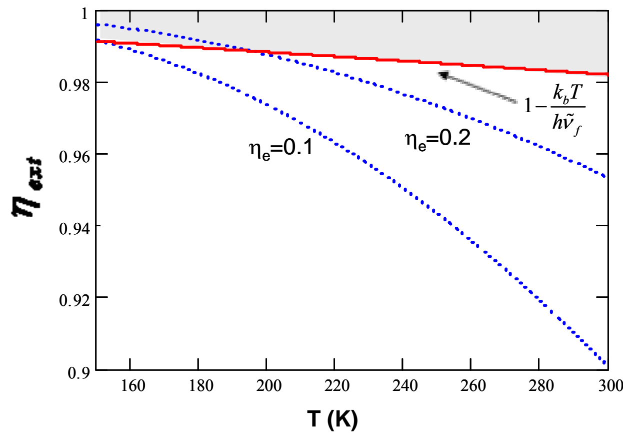

Fig. 3 The required external quantum efficiency (EQE) as a function of temperature for GaAs under typical parameters.

This indicates that, for example at T=150 K, the break-even lifetime is lowered by ~ 40 times compared with the room temperature (T=300 K) condition. This is further depicted in Fig. 3 where the η_{ext} is plotted versus T for two values of η_e, which define the range of a nearly index matched dome. The solid red line indicates the break-even condition described by Eq. (16). This condition together with the fact that A (typically dominated by surface recombination) increases inversely with temperature [27, 28], makes the low temperature observation of laser cooling more favorable although the efficiency (≈kT/E_g) decreases linearly. The reduction in cooling efficiency is primarily due to the reduction of the electron-phonon absorption probability at lower temperatures. In particular, the population of LO phonons vanishes as manifest in the reduction of exciton linewidth Γ described by [14]:

$$\Gamma(T)=\Gamma_0+\sigma T+\gamma N_{LO}(T) \quad (18)$$

where Γ_0 is due to impurities as well as inhomogeneous broadening, σ accounts for the contribution of acoustic phonons, and γ is the coefficient of LO-phonon scattering with $N_{LO}(T)$ denoting the corresponding Bose-Einstein phonon distribution. For the exciton densities involved, we can ignore possible broadening due to exciton-exciton scattering [29]. As the lattice temperature approaches 10 K, the acoustic phonon contribution begins to dominate. At such low temperatures, however, the exciton-phonon scattering rate ($\approx\Gamma$) becomes comparable to the radiative recombination rate (BN^2) and consequently cold exciton recombination occurs before complete thermalization with the lattice. Similar processes, related to premature hot exciton recombination, have also hindered experimental observation of Bose-Einstein condensation in semiconductors. This problem is significantly alleviated by employing quantum confined systems where σ is enhanced by nearly 3 orders of magnitude. This relaxes wave-vector conservation along the confinement directions [30]. Enhanced cooling in quantum confined systems may allow operation at temperatures < 10 K.

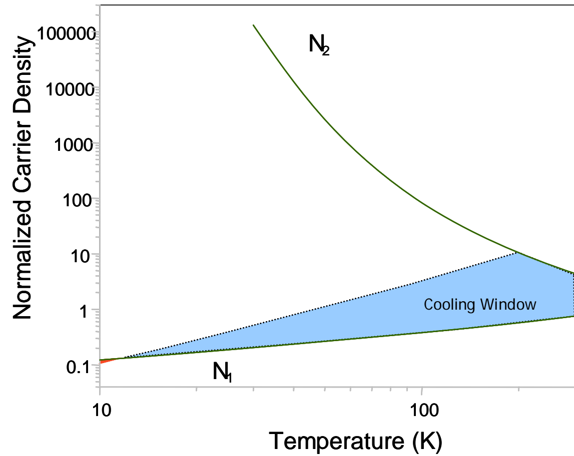

Fig. 4 The upper carrier density N_2, given by Eq. (14) is seen to be unattainable in GaAs due to band-blocking as temperature is lowered below 200 K. We assumed a band-tail excitation at $h\nu = h\nu_f - kT$.

Another issue of concern is the role of Pauli band-blocking and other many-body interactions. Band-blocking may be a limiting factor for long wavelength excitation where the low density of states gives rise to a stronger bleaching of the interband absorption. It is therefore necessary to have a good understanding of the absorption and emission spectra and its dynamic nonlinearities. Theoretical models exist that deal with absorption spectra of semiconductor structures under various carrier densities and lattice temperatures. While they vary in their complexity, almost all existing theories (for 2D and 3D systems) are so-called "plasma theories" where the effect of Coulomb screening is taken into account assuming that the photogenerated carriers form an e-h plasma.[31-33] Recently, more rigorous and computationally intensive theories that employ exciton Hamiltonians as their starting point have been considered for 1D systems [34]. We postpone further discussion on the precise role of band-blocking and many body issues to future publications and turn our attention to the more pressing issue of the external efficiency.

In the simple two-parabolic band approximation, the effect of band-blocking is shown in Fig. 4 where the condition $f_c = f_v$ sets a new upper density N_2 which is far smaller than that given by Eq. (14) at low temperatures. According to this simple model (which also ignores the favorable T dependence of the A coefficient), the new cooling window vanishes at $T\approx 10$ K.

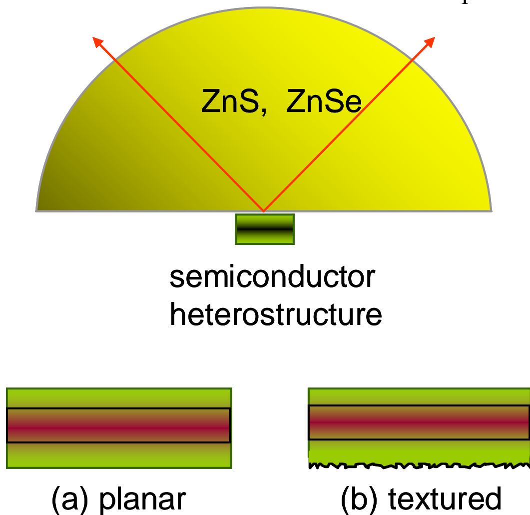

Fig. 5 Two possible structures that use a high-index dome for increasing luminescence escape efficiency: (a) polished planar, and (b) surface textured heterostructures.

We analyze the effect of radiation trapping and photon recycling in laser cooling in GaAs. We consider two structures that have been suggested for improving the efficiency of LEDs where the luminescence escape is facilitated by use of a nearly index matched dome attached to the heterostructure as depicted in Fig. 5 [11]. In the first case (a), the thin heterostructure layer is polished thus limiting the escape cone to that determined by the total internal reflection. In the second case (b), a textured-surface layer is assumed that effectively randomizes the photon trajectories and hence further increases the escape efficiency via photon recycling. Ignoring resonant cavity

effects, the escape probabilities in both cases been evaluated with statistical geometric optics for LEDs using summation of intensities with proper solid-angle averaging in a photon-gas model [35]. Using the thickness (L) of the GaAs as a parameter, we analyze these systems assuming a dome material of index n_d=2.4 for ZnS. ZnS is chosen for its extremely low optical loss within the spectral region of interest.

To evaluate the luminescence spectrum, R(ν), we use an analytical plasma theory that has shown good agreement with experimental results for T > 70 K [31, 32]. The absorption spectra contains contributions from Coulomb screened bound and free excitons in a bulk semiconductor:

$$\alpha_0(N,\nu) = a_0 \sum_n \frac{1}{n}\left[\frac{1}{n^2} - \frac{n^2}{g^2}\right]\delta_\Gamma\left[\frac{h\nu - E_n}{E_0}\right] + a_0 \int_0^\infty dx \frac{\sinh(\pi g\sqrt{x})}{\cosh(\pi g\sqrt{x}) - \cos(\pi\sqrt{4g - xg^2})}\delta_\Gamma\left[\frac{h\nu}{E_0} - x\right], \quad (19)$$

where a_0 is a material constant, g is an screening parameter, E_0 is the exciton Rydberg energy, E_n is the n-exciton energy, Γ is the exciton linewidth and δ_Γ is a broadened delta function . Calculated absorption α(ν) and luminescence S(ν) spectra using Eqs. (19) and (5) are shown in Fig. 6. These results are then used to obtain escape efficiency (η_e) and escaped mean luminescence energy $h\tilde{\nu}_f$ (normalized to the bandgap) as a function of the thickness of the GaAs (hetero-)structure is shown in Fig. 7. Photon recycling due to the textured-surface structure results in much higher escape efficiency as the thickness is reduced. This enhanced efficiency is obtained at the expense of higher red shifting of the luminescence because lower energy photons suffer less absorption and can eventually escape. The polished (planar) surface case, however, is relatively constant for thicknesses up to 1 μm; the luminescence photon energy remains close to the internal value of $h\nu_f$. We conclude that while photon recycling mechanism is a useful tool for increasing the efficiency of LED's, it may be detrimental for laser cooling due to luminescence red-shifting. To quantify this statement and for the sake of comparison, we assume that the excitation energy is fixed at $h\nu = h\nu_f - kT$ and then use Eq. (7) to define a normalized cooling power as:

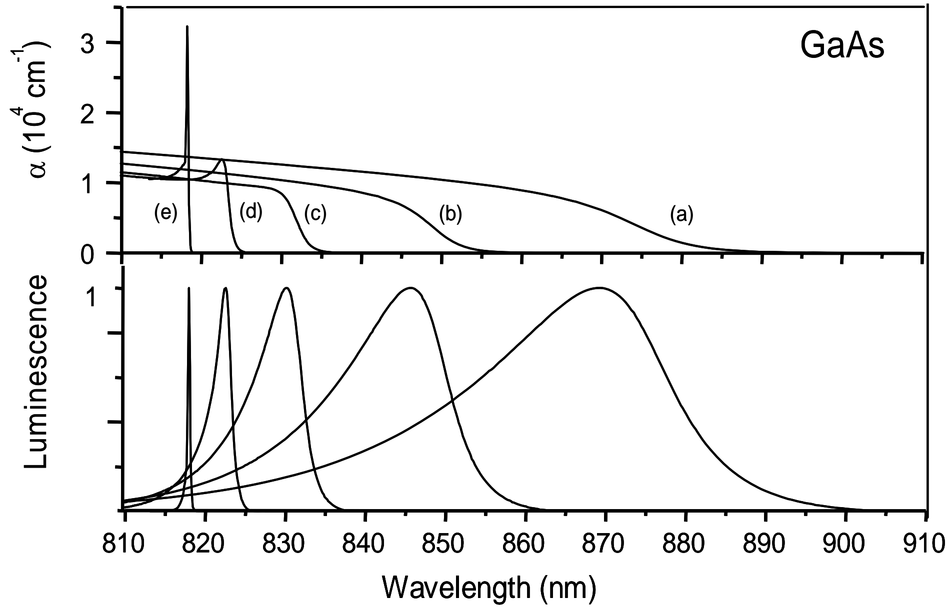

Fig. 6 Calculated spectra of absorption (top), luminescence (bottom) for GaAs in 5 different cases: e) T=10 K, N=2×10^{15} cm^{-3} ; d) T=70 K, N=2×10^{16} cm^{-3}; c) T=120 K, N=1×10^{17} cm^{-3} ; b) T=200 K, N=3×10^{17} cm^{-3}; and a) T=300 K, N=5×10^{17} cm^{-3}

$$\overline{P}_c = K\eta_e(h\tilde{\nu}_f - h\nu)V = K\eta_e(kT - \Delta\varepsilon)V \quad (20)$$

where K is a normalization constant, $\Delta\varepsilon = h\nu_f - h\tilde{\nu}_f$ is the amount of luminescence photon energy shift, and V=Area×L is illumination /recombination volume. We evaluated this quantity ($\overline{P}_c$) for the two structures as a function of the thickness. To achieve the highest cooling power and lowest temperature, the planar structure with a thickness of 0.75-1.5 μm offers an optimum geometry. On the other hand, if we desire the highest cooling efficiency, and/or a large η_e is required to overcome the break-even condition, then thin (L < 500 nm) and textured-surface structures are advantageous. Another factor that restricts the thickness is surface recombination. Experiments show that surface recombination becomes dominant in our GaAs/GaInP heterostructures at L<500 nm.

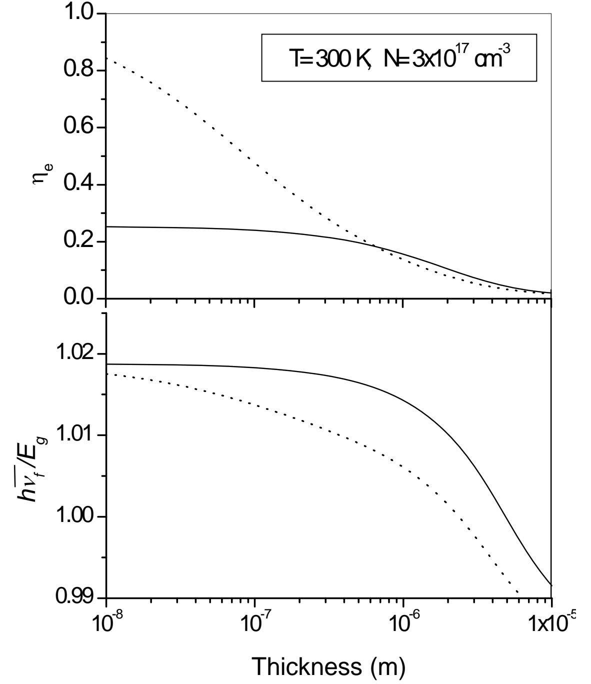

Fig. 7 The calculated escape efficiency and escaped mean luminescence photon energy as a function of the GaAs thickness for the structures (a)-solid line and (b)-dotted line as described in Fig. 5.

3. EXPERIMENTS

Anti-Stokes luminescence can easily be observed in a high quality direct gap semiconductor, as shown in Fig. 8 for GaAs. Achieving net cooling, however, requires that we satisfy the inequality described by Eq. (16). For a given material, the parameters B and C are fixed and can only be altered by varying the samples temperature. The controllable parameters are A, η_e and α_b. The A parameter is primarily due to surface recombination that varies drastically depending on the growth technique and environment. Lowest surface recombination velocities have been achieved in GaAs/GaInP double heterostructures grown by the MOCVD technique. We have extensively studied GaAs heterostructure systems and characterize their nonradiative lifetime (τ_{nr}=1/A) and external quantum efficiency (EQE) for various growth techniques as a function of temperature and active-layer thickness.[26] We have also investigated various techniques for enhancing luminescence extraction efficiency (η_e).[36, 37]. In addition to Gauck et al's initial experimental work, other relevant experimental investigations include that of the group in the University of New South Wales, Australia. [38, 39]. In 1999, Finkeissen et al reported an observation of laser induced local cooling in GaAs/AlGaAs multiple quantum wells at cryogenic temperatures.[10]. Upon close examination of the experimental conditions and the method by which the authors deduced temperature change, we strongly believe that no lattice cooling could have been observed under their conditions. The luminescence shift that was interpreted as a consequence of lattice cooling can be explained by population effects leading to exciton screening and/or a phonon absorption bottleneck.

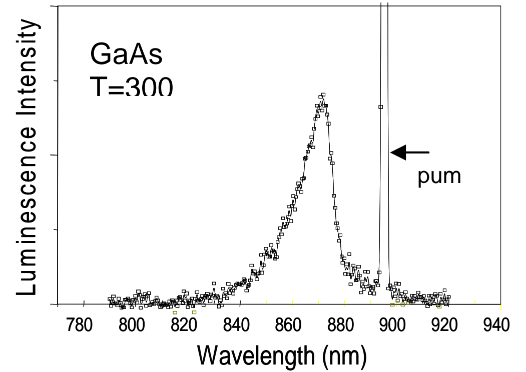

Fig. 8 Laser Induced anti-Stokes luminescence observed in GaAs/GaInP double heterostructure.

The following section contains a summary of some of our experimental investigations toward the first demonstration of laser cooling in a semiconductor.

3.1 Characterization of nonradiative lifetime

Time resolved photoluminescence (PL) is used to measure the nonradiative recombination lifetime (1/A) as a function of temperature in GaAs heterostructures. We compare GaAs/GaInP heterostructures grown by MOCVD with MBE-prepared GaAs/AlGaAs structures. The results indicate that MOCVD produces higher quality hetero-surfaces with much lower surface recombination velocity (Figure 10). The luminescence lifetimes shown in Fig. 10 for the GaAs/GaInP structures are dominated by impurity-mediated radiative recombination. The nonradiative component of the decay is deduced by fitting the temperature dependence of the decay by:

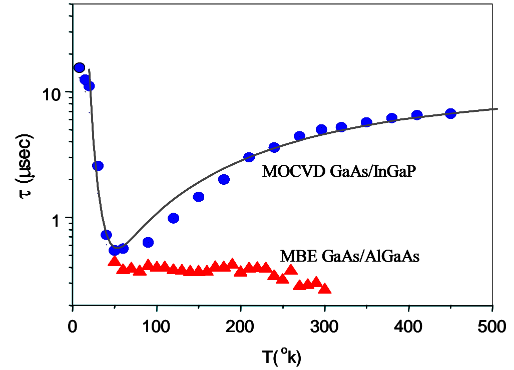

Fig. 10 Photoluminescence lifetime measured as a function of temperature for two types of GaAs heterostructures.

$$\frac{1}{\tau_{PL}} = \eta_e B(T) N_A^-(T) + A(T) \quad (21)$$

where N_A^- is the ionized acceptor density. Since the temperature dependence of the B and N_A^- are well known, A(T) (or in some cases an its upper limit) can be extracted from these experiments.

The effects of epitaxial lift-off and bonding of the heterostructures onto the ZnS or ZnSe dome lenses were also investigated. We have reported an interface recombination velocity of 0.6 cm/s (at T=300 K) in a 1µm thick GaAs/GaInP heterostructure before lift-off. This is the lowest interface velocity ever reported for such materials. After liftoff (wet etching of the AlAs layer) and van der Waals bonding the structures to the dome materials (ZnS), we find that the nonradiative rate increases as shown in Fig. 11. We attribute this to the bending induced dislocations during the processing. We are currently refining our fabrication processes, and are developing techniques to minimize bending that degrades the interface prior to bonding.

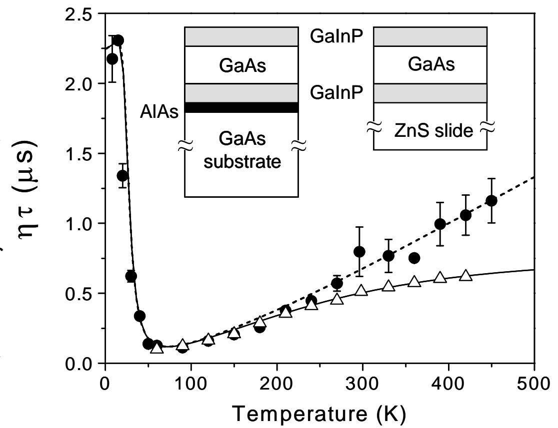

Fig. 11 Photoluminescence lifetime of GaInP/GaAs d=1.0 µm heterostructures before lift-off (circles) and after lift-off and bonding to a ZnS slide (triangles). The dotted curve is from a model that ignores interface recombination; solid curve includes interface recombination. Inset top-left: Schematic of unprocessed sample; Inset top-right: After lift-off and bonding to ZnS. Bottom:

3.2 External Efficiency and Luminescence Removal

3.2 External Efficiency and Luminescence Removal. Trapped luminescence effectively inhibits radiative recombination; this is accounted for with the term $\eta_e B$. The extraction efficiency η_e can be enhanced, in principle, through "photon recycling", a practice that is well known in LED engineering. Photon recycling is the process of luminescence absorption and re-emission in multiple sequences. It is only partially effective in a laser cooling application, however, because of the tendency for the net luminescence to shift toward longer wavelengths. Cooling is inhibited when the mean luminescence wavelength approaches the pump wavelength.

Most of the luminescence is trapped because of total internal reflection. This is caused by the high refractive indices of semiconductors (n ≈ 3.6 near the band edge of GaAs). Only about 2% of the light emanating from the irradiated volume bounded by vacuum can escape. Light rays must propagate nearly normal to the heterostructure surface to avoid total internal reflection. This means that the vast majority of the luminescence is reflected back into the semiconductor where it can cause heating.

Luminescence trapping caused by total internal reflection also hinders LED performance. To address this, LED's have a coupling lens between the semiconductor and vacuum.

The lens material has a refractive index close to the semiconductor. In an LED application, absorption heating in the lens is of little consequence. When a dome lens is used in laser cooling, absorption becomes critical (Fig. 5-top)[11]. Isotropically emitted luminescence passes into the dome and reaches the curved surface at nearly normal incidence. These rays are not subject to total internal reflection and can escape. We have made a thorough study of candidate lens materials and determined that ZnSe and particularly ZnS have acceptable transmission and refractive index relatively close to GaAs [37]. Such dome lenses will increase the output coupling efficiency by an order of magnitude compared to a semiconductor-vacuum interface. This is a direct consequence of the fact that refraction across the interface can be accomplished for a wider range of incidence angles. In Fig. 6 (top), pump light enters the heterostructure from the bottom surface. Very little luminescence can escape at this surface because of the substantial index mismatch between the semiconductor and vacuum. We have studied texturing of the bottom surface (Fig 6-b) to randomize photon trajectories, which allows a statistically larger number of photons to strike the upper surface at angles smaller than the critical angle and escape. The trade-off here is increased propagation path in the heterostructure leading to deleterious photon recycling and red-shifting. Our analysis shows that surface texturing is beneficial in very narrow GaAs layers (< 200 nm) [8].

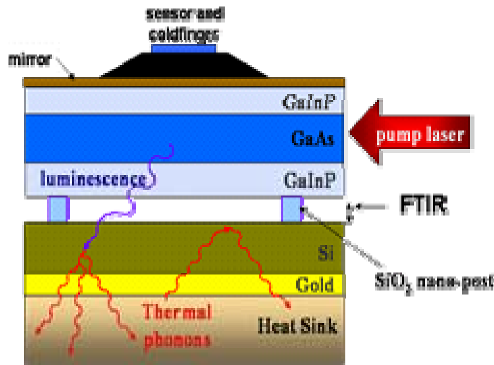

Fig.12 The concept of “nanogap”: luminescence couples out by frustrated total internal refraction (FTIR); the vacuum nanogap maintains a thermal barrier.

The Nanogap: A completely different and novel approach to the luminescence output coupling problem that we are investigating is to replace the dome lens with a sub-micron vacuum gap between the heterostructure and absorbing substrate such as silicon. This concept is depicted in Fig. 12.[36] If the gap space is less than 100 nm, luminescence rays striking the surface at all angles can couple to the absorbing substrate via an evanescent wave. Optical energy is transferred to the absorber, which remains in thermal isolation from the heterostructure because of the vacuum gap. Our analysis shows that luminescence outcoupling surpasses the ZnS dome lens scheme for a gap separation < 50 nm. Registration of the two surfaces is accomplished by fabricating a small number of insulating posts grown from oxide, nitride, or randomly deposited nano-particles.

3.2 Measurements of External Quantum Efficiency (EQE): Following Gauck et al, [11], we obtain EQE or η_{ext} by performing a measurement of the laser induced cooling/heating efficiency versus the pump wavelength. As indicated by Eq. (12), taking $\eta_{abs}\approx 1$ (valid for short wavelengths), η_{ext} is obtained by taking the ratio of the escaped mean luminescence wavelength (λ_f) to the extrapolated wavelength corresponding to the temperature zero-crossing (η_c=0). The measurement is performed under constant carrier density which is monitored by keeping the luminescence signal (spectral peak or area) constant as the pump wavelength is varied. The fractional heating of the sample versus the wavelength is therefore proportional to the cooling efficiency η_c. Noncontact temperature measurement of the sample is desirable to minimize parasitic heating that may result from thermocouple attachments [11]. We developed an excite-probe differential luminescence thermometry (DLT) technique that accurately deduces the temperature variations by monitoring the bandgap luminescence. This technique uses a constant weak probe laser for inducing luminescence used for temperature sensing. It therefore requires a delicate time gating to distinguish this luminescence from the strong pump-induced luminescence. Furthermore, this technique is adaptable to performing EQE measurements at cryogenic temperatures where other non-contact temperature measurements (such as thermal cameras) have no longer sufficient sensitivity.

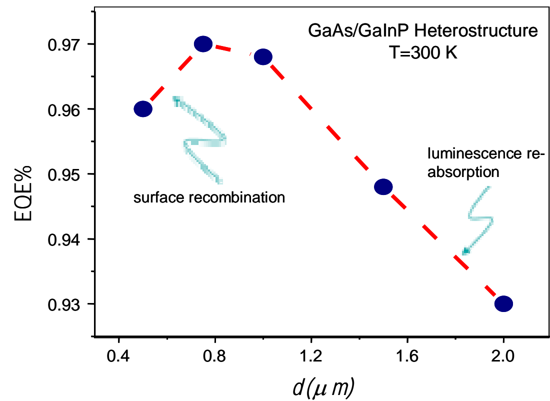

Fig. 13 Measured EQE (η_{ext}) as a function of the GaAs thickness in the GaAs/GaInP double heterostructures.

We have performed some preliminary measurements of EQE for various sample thicknesses and temperatures. At room temperature, the effect of active layer thickness on EQE was measured for GaAs/GaInP double heterostructure as shown in Fig. 13. We found that the optimum thickness of GaAs is about 0.8 μm. The degradation of the EQE at higher thicknesses is understood in terms of diminishing $\eta_e \propto \exp(-\alpha d)$ due to luminescence re-absorption. As the thickness is lowered, the non-radiative decay rate $A=2S/d$ (with S denoting the surface recombination velocity), is enhanced since carriers can take shorter time to diffuse to surface and recombine through surface states. It should be noted that as described by Eq. (11), for a given sample (thickness), η_{ext} has to be maximized by adjusting the laser power to inject the optimum carrier density.

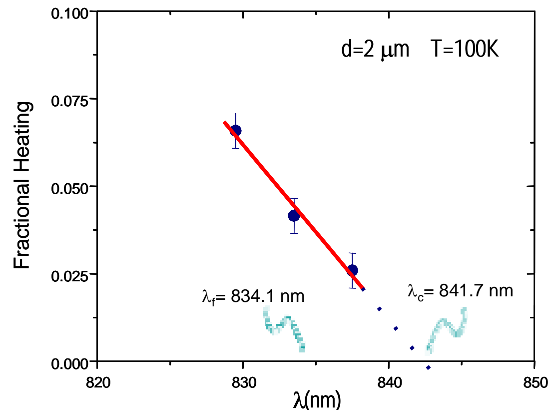

Fig. 14 Fractional heating measured in GaAs/GaInP double heterostructure as a function of pump wavelength while keeping the carrier density constant.

Our latest experiments involve measurement of EQE at low temperatures using the differential luminescence thermometry. As described in section 2 and depicted in Fig. 3, EQE gets enhanced at low temperatures. Net cooling may be achieved if parasitic absorption can also be reduced to an acceptable level. Our preliminary results (Fig. 14) exhibit an EQE of 99% measured at T=100 K for 2 μm thick GaAs/GaInP double heterostructure. To our knowledge, this is the highest EQE ever reported for a semiconductor. Experiments are currently underway to measure EQE at low temperatures for optimally thick samples of 0.75 μm as shown in Fig. 13. With improved fabrication and preparation (sample cleaning) techniques, we can reduce the background absorption to levels that net cooling can be observed in these systems.

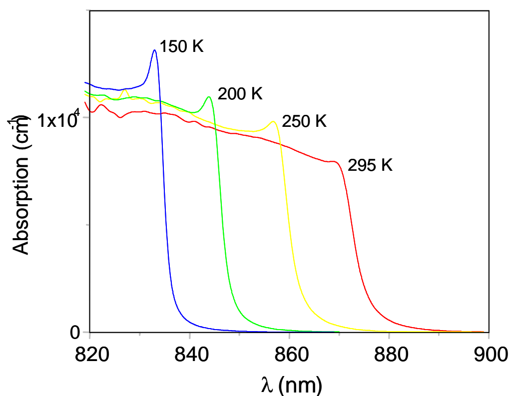

Fig. 15 Absorption spectra obtained using reciprocity (KMS relation) from the corresponding photo-luminescence measured at various temperatures.

Laser cooling in semiconductors relies on band-tail (Urbach tail) excitation, so quantifying this parameter is of great significance. For our thin samples, direct measurement of the absorption coefficient is not possible. Absorption may be obtained using photoluminescence excitation (PLE) with reciprocity; luminescence spectra are converted to absorption spectra by using the KMS relation of Eq. (5). We present here the results of using this approach to characterize GaAs at various temperatures. The deduced absorption spectra are shown in Fig. 15 for temperatures ranging from 150K to room temperature. Intriguing exciton-like absorption peaks appear at the band edge at low temperatures. The luminescence spectra are recorded at low injected carrier density so the emergence of exciton peaks is not unexpected. Note that the theoretical results shown in Fig. 6 do not exhibit pronounced excitonic features until T<100 K due to Coulomb screening at relatively high carrier densities used for those calculations.

In summary, we have developed a model to treat laser cooling in semiconductors under arbitrary external efficiency. Break-even conditions and requirements in terms of nonradiative lifetime and luminescence extraction efficiency are obtained. The latest experimental results were reviewed and various device geometries described to elucidate necessary experimental conditions for observing laser cooling in GaAs.

4. ACKNOWLEDGEMENTS

The authors gratefully acknowledge the support from the Air Force Office of Scientific Research (Grants F49620-0201-0059 and F49620-02-1-0057), and Multidisciplinary University Research Initiative (MURI) grant FA9550-04-1-0356 under the Consortium for Laser Cooling in Solids (CLCS). We also acknowledge the National Aeronautics and Space Administration (Grant NAG5-10373), and NSF's IGERT program under Cross-disciplinary Optics Research and Education (CORE) grant. This work was carried out in part under the auspices of the U.S. Department of Energy.

5. REFERENCES

[1] P. Pringsheim, Z. Phys. 57, 739 (1929).

[2] R. I. Epstein, M. I. Buchwald, B. C. Edwards, et al., Nature 377, 500 (1995).

[3] J. L. Clark and G. Rumbles, Physical Review Letters 76, 2037 (1996).

[4] B. C. Edwards, J. E. Anderson, R. I. Epstein, et al., in *Cryocoolers 11* (Plenum Press New York, 2000).

[5] B. C. Edwards, J. E. Anderson, R. I. Epstein, et al., Journal of Applied Physics 86, 6489 (1999).

[6] R. I. Epstein, J. E. Anderson, and B. C. Edwards, in *OSA Annual Meeting*, Providence, RI, 2000), p. paper ThDD2.

[7] T. R. Gosnell, Optics Letters 24, 1041 (1999).

[8] C. Hoyt, M. Hasselbeck, M. Sheik-Bahae, et al., J. Opt. Soc. Am. B 20, 1066 (2003).

[9] C. W. Hoyt, M. SheikBahae, R. I. Epstein, et al., Physical Review Letters 85, 3600 (2000).

[10] E. Finkeissen, M. Potemski, P. Wyder, et al., Applied Physics Letters 75, 1258 (1999).

[11] H. Gauck, T. H. Gfroerer, M. J. Renn, et al., Applied Physics a-Materials Science & Processing 64, 143 (1997).

[12] A. N. Oraevsky, J. Russian Laser Research 17, 471 (1996).

[13] L. A. Rivlin and A. A. Zadernovsky, Optics Communications 139, 219 (1997).

[14] P. K. Basu, *Theory of optical processes in semiconductors : bulk and microstructures* (Clarendon Press ; Oxford University Press, OxfordNew York, 1997).

[15] J. I. Pankove, *Optical processes in semiconductors* (Prentice-Hall, Englewood Cliffs, N.J.,, 1971).

[16] M. Born and E. Wolf, *Principles of optics : electromagnetic theory of propagation, interference and diffraction of light* (Cambridge University Press, Cambridge ; New York, 1999).

[17] P. Asbeck, Journal of Applied Physics 48, 820 (1977).

[18] W. van Roosbroeck and W. Shockley, Phys. Rev. 94, 1558 (1954).

[19] S. L. Chuang, *Physics of optoelectronic devices* (Wiley, New York, 1995).

[20] E. Yablonovitch, T. J. Gmitter, and R. Bhat, Phys. Rev. Lett. 61, 2546 (1988).

[21] J. M. Olson, R. K. Ahrenkiel, D. J. Dunlavy, et al., Appl. Phys. Lett. 55, 1208 (1989).

[22] A. Haug, Semiconductor Science and Technology 7, 373 (1992).

[23] H. Yi, J. Diaz, B. Lane, et al., APPLIED PHYSICS LETTERS 69, 2983 (1996).

[24] C. W. Hoyt, W. Ptterson, M. P. Hasselbeck, et al., in *Quantum Electronics and Laser Science (QELS)* (OSA, Baltimore, 2003), Vol. Paper QTHL4.

[25] G. P. Agrawal and N. K. Dutta, *Long-wavelength semiconductor lasers* (Van Nostrand Reinhold, New York, 1986).

[26] B. Imangholi, M. P. Hasselbeck, M. Sheik-Bahae, et al., Applied Physics Letters 86, 81104 (2005).

[27] G. W. Thooft and C. Vanopdorp, Appl. Phys. Lett. 42, 813 (1983).

[28] R. K. Ahrenkiel, J. M. Olson, D. J. Dunlavy, et al., J. Vacuum Science & Tech. A 8, 3002 (1990).

[29] A. C. Schaefer and D. G. Steel, Physical Review Letters 79, 4870 (1997).

[30] L. V. Butov, C. W. Lai, A. L. Ivanov, et al., Nature 417, 47 (2002).

[31] L. Banyai and S. W. Koch, Zeitschrift Fur Physik B-Condensed Matter 63, 283 (1986).

[32] H. Haug and S. W. Koch, *Quantum theory of the optical and electronic properties of semiconductors* (World Scientific, Singapore, 1994).

[33] J. P. Lowenau, F. M. Reich, and E. Gornik, Physical Review B-Condensed Matter 51, 4159 (1995).

[34] T. Meier and S. W. Koch, Semiconductors and Semimetals 67, 231 (2001).

[35] I. Schnitzer, E. Yablonovitch, C. Caneau, et al., Applied Physics Letters 62, 131 (1993).

[36] R. I. Epstein, B. C. Edwards, and M. Sheik-Bahae, U.S., 2002).

[37] B. Imangholi, M. P. Hasselbeck, and M. Sheik-Bahae, Opt. Comm. 227, 337 (2003).

[38] K. R. Catchpole, K. L. Lin, P. Campbell, et al., Semiconductor Science and Technology 19, 1232 (2004).

[39] K. L. Lin, K. R. Catchpole, P. Campbell, et al., Semiconductor Science and Technology 19, 1268 (2004).